Malaysian Journal of Analytical Sciences (MJAS)
Published by Malaysian Analytical Sciences Society

IMPROVING THE MORPHOLOGICAL, THERMAL, AND ACOUSTICS PROPERTIES OF POLYURETHANE-UREA BIOFOAM USING INDUSTRIAL PLYWOOD SAWDUST WASTE

(Meningkatkan Morfologi, Termal dan Sifat Akustik Busa Poliuretan-Urea Menggunakan Sisa Habuk Papan Kayu Lapis)

Herlina Nofitasari[1]*, Ari Handono Ramelan[2], Mohammad Masykuri[3]

[1]Master's Degree Program in Environmental Science
[2]Faculty of Mathematics and Natural Sciences
[3]Faculty of Teacher Training and Education
Universitas Sebelas Maret, Surakarta 57126, Indonesia

**Corresponding author: henosa25@gmail.com*

Received: 29 December 2021; Accepted: 27 February 2022; Published: 27 June 2022

Abstract

Majority of the polyurethane–urea (PUU) foam is made from petroleum raw materials. Concerns regarding the loss of petroleum resources promote the environmentally sustainable manufacture of foam. The production of PUU foam synthesis from natural materials and waste composites was then developed. The PUU/industrial plywood sawdust waste (IPSW) biofoam was synthesized from a mixture of polyethylene glycol (PEG), methylene diisocyanate (MDI), ethylenediamine (EDA), maleic anhydrate (MAH), and IPSW by using a one-shot method. 5% IPSW was applied to the composition of the synthesized biofoam and the MDI ratio was increased. Fourier Transform Infrared Spectroscopy (FTIR) was used to identify functional groups of biofoam. The pore morphology of the biofoam was observed with Microscope Camera and Scanning Electron Microscopy (SEM), the thermal ability was measured with Thermogravimetric Analysis (TGA), and the sound absorption ability was measured by using a two-microphone impedance tube according to the ASTM E-1050 standard. Based on FTIR spectra identification, the biofoam contains OH, CH, CO, and NH chemical groups. The results reveal that the PUU/IPSW biofoam had intermediate macropore morphology (closed and open cells), thermal resistance above 120^{o}C, and potential materials as sound-absorbing. The improvement in the biofoam properties upon the addition of organic filler shows that the biofoam is promotable as renewable material. This study suggests better formulation design to enhance the biofoam property performance.

Keywords: acoustics, polyurethane-urea foam, sawdust, scanning electron microscopy, thermogravimetric analysis

Abstrak

Kebanyakan busa poliuretan-urea (PUU) diperbuat daripada bahan mentah petroleum. Kebimbangan mengenai kehilangan sumber petroleum menggalakkan pembuatan busa yang mampan secara alam sekitar. Penghasilan sintesis busa PUU daripada bahan alam dan komposit sisa telah dibangunkan. Busa PUU telah disintesis daripada campuran polietilen glikol (PEG), metilen diisosianat (MDI), etilen diamin (EDA), maleat anhidrat (MAH), dan sisa habuk papan industri kayu lapis (IPSW) dengan menggunakan kaedah satu pukulan. Lima peratus IPSW telah digunakan pada komposisi biofoam tersintesis dan nisbah MDI

telah meningkat. Spektroskopi Infra-Merah Transformasi Fourier (FTIR) digunakan untuk mengenal pasti struktur biofoam. Morfologi liang biofoam diperhatikan menggunakan mikroskop kamera dan SEM, TGA untuk pengukuran haba, dan keupayaan biofoam untuk menyerap bunyi diukur menggunakan tabung impedansi dua mikrofon mengikuti standar ASTM E-1050. Berdasarkan pengenalpastian spektrum FTIR, biofoam mengandungi kumpulan kimia OH, CH, CO, dan NH. Keputusan menunjukkan bahawa biofoam PUU/IPSW mempunyai morfologi makropori perantaraan (sel tertutup dan sel terbuka), rintangan haba melebihi 120 ^{o}C, dan berpotensi menjadi bahan penyerapan bunyi. Kemajuan kinerja ketika ditambahkan pengisi organik menunjukkan bahawa ini dapat dipromosikan sebagai bahan terbarukan. Studi ini menyarankan agar membuat formulasi yang lebih baik untuk meningkatkan prestasinya.

Kata kunci: akustik, busa poliuretan-urea, habuk papan, mikroskopi imbasan elektron, analisis termogravimetrik

Introduction

Population growth and rapid transportation progress have led to environmental problems in the community, including noise pollution. The effects are severe for those who have been exposed, both physically and mentally. This condition can be regulated by using sound-absorbing materials. There are two types of sound-absorbing materials: resonant and porous sound-absorbing materials. The morphology of the latter is made up of channels, gaps, and holes that allow sound waves to pass through [1-3].

Foam is a porous material that can be used to absorb sound. The foam production is synthesized from diols and polyols i.e. polyurethane chemical compounds [2, 4]. Polyurethanes are widely used for other applications such as paints, jacket coatings, elastomers, insulators, elastic fibers, and leather equipment. Polyurethane production and demand projections rose through 2020 [5]. The production of polyurethane foam is incompatible with sustainable development because it uses petroleum as raw material. Therefore, it is necessary to find alternative raw materials that are less harmful to the environment.

Renewable polyol modification is developed in the production of polyurethane by using biomass as raw material through oxypropylation or acid liquefaction process. The production of bio-polyol using oxypropylation method includes the use of palm oil, *Sapium sabiferum* oil, castor oil, soybean oil, grapeseed oil, sunflower oil, tung oil and canola oil. The current bio-polyol production process using liquefaction acid is derived from eucalyptus and pine woods, bamboo, Cellulose nanofibrils, Yaupon holly (*Ilex vomitoria*), sugar-cane bagasse, bagasse, and jute fiber. Both processes can produce environmentally friendly polyurethane foam raw materials [4-8].

In addition to bio-polyols, the use of isocyanate alternatives such as Non-isocyanate polyurethane (NIPU), which is derived from mimose tannins [9], lysine, sorbitol, vegetable oils, and other sources, is another way to keep polyurethane foam production sustainable. Recycling polyurethane foam [4] and integrating natural waste materials into the production process are also green choices. Natural fiber blends of various concentrations and thicknesses in polyurethane foam composites have varied sound absorption capabilities [10]. The addition of *Shorea leprosa* wood fibers to the polyurethane foam affects its acoustic performance [11]. Production of biofoam from polyurethane-urea blends with various concentration of industrial plywood sawdust has a good sound absorption coefficient [12].

It was reported that polyurethane foam composites containing nanosilica and nanosilica solution at an optimum level of 2 wt.% had a negative impact on foam cell morphology, and the TGA test results for rigid polyurethane foam composites containing 1 wt.% nanosilica solution had poor thermal resistance [13]. As compared to foams without the addition of halloysite nanocomposites, rigid polyurethane foam with palm oil as raw material and halloysite nanocomposite had stable thermal resistance, and SEM results showed a smooth cell surface structure and larger cell size [2]. Polyurethane foam synthesized with clove composites (*Syzygium aromaticum*) at various concentrations had rheological behavior, cellular

structure, and further mechanical & thermal performance of the modified material [8].

The other research studied polyurethane foam with addition of diatomite and hydroxyapatite. The thermal degradation of diatomite porous polyurethane foam biocomposites was lower than that of hydroxyapatite porous polyurethane foam biocomposites. Diatomite and hydroxyapatite increase the surface area of the polyurethane foam and harden the pores [14]. Rigid foam made by combining non-isocyanate polyurethane (NIPU) tannins with addictive glutaraldehyde and citric acid had the same morphology, called Open-Cell, but the number of cell wall pores decreased as glutaraldehyde was added, while citric acid increased the number of foam cells. The thermal resistance of the NIPU foam in all compositions was the same except for the composition of 2 grams of hexamine and 6 grams of citric acid which was higher at a temperature of 790 ^{o}C and a residue of 18.7% [9].

This research described the synthesis of polyurethane-urea (PUU) biofoam with industrial plywood sawdust waste composites (IPSW). The PUU/IPSW biofoam was synthesized by adding a chain extender in the form of ethylene diamine (EDA), coupling agent in the form of maleic anhydrate (MAH), and industrial plywood sawdust waste as filler. The chain extender is a low molecule containing an amine group at the end that plays a major role in polymer morphology. The addition of a chain extender and diisocyanate provided a wide range of hard segment characteristics and the physical performance of polyurethane. The morphological structures were characterized by SEM and Microscope Camera. Meanwhile, thermal ability was analyzed by TGA, and acoustics test was conducted through impedance tube.

Materials and Methods

Materials

The materials used to synthesize the PUU/IPSW biofoam were chemical compounds and biomass. The chemical compounds included polyethylene glycol (PEG) 400 (Polyol), 4.4'-diphenylmethane diisocyanate (4.4'-MDI), ethylenediamine (EDA), and maleic anhydrate (MAH) while the biomass was in the form of industrial plywood sawdust waste (IPSW). The detail of various compositions of the PUU/IPSW biofoam are shown in Table 1.

Sample preparation

The biofoam was synthesized by using a one-shot method. This method worked by combining all of the ingredients until they were fully homogeneous, as detailed in Figure 1. First, the polyol and diisocyanate were mixed and stirred. Then, the chain extender (EDA), the coupling agent (MAH), and the IPSW filler were added. The composition of the ingredients was calculated by the mass ratio. The samples were coded as BP0, BP1, BP2, BP3, BP4, and BP5 for the PUU/IPSW biofoam with 0%, 1%, 2%, 3% , 4%, and 5% IPSW respectively with a ratio of PEG:MDI (1:1), and BP1.5 for the PUU/IPSW biofoam of 5% with a ratio of PEG:MDI (1:1.5).

Table 1. Variation of the PUU/IPSW biofoam composition

Samples	PEG (g)	MDI (g)	EDA 0.1% (g) (w/w)	MAH 0.01% (g) (w/w)	Waste % (g) (w/w)
BP0	15	15	0.3	0.03	0
BP1	15	15	0.3	0.03	0,31
BP2	15	15	0,3	0.03	0,62
BP3	15	15	0,3	0.03	0,94
BP4	15	15	0,3	0.03	1,26
BP5	15	15	0,3	0.03	1,6
BP1,5	15	22,5	0.3	0.03	1,6

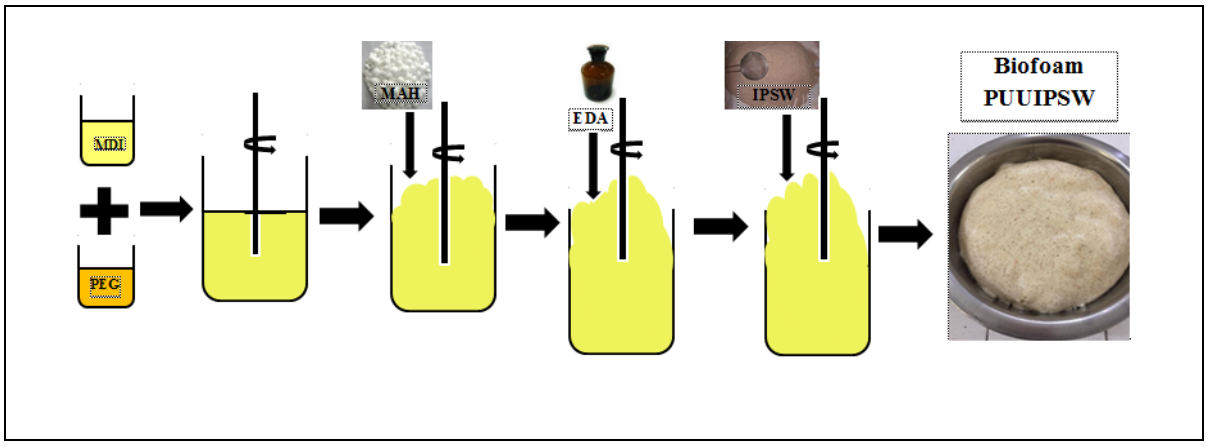

Figure 1. Procedural scheme for the PUU/IPSW biofoam synthesis

Microscope camera

The biofoam pore morphology in was observed by using a Nikon Eclipse 80i microscope camera for 10x magnification. The resulted pore distribution was calculated by using Image J software. The pore distribution data were analyzed by using OriginLab software.

Scanning Electron Microscopy

The morphological properties of biofoam cells were observed by using Scanning Electron Microscopy (SEM) Phenom ProX. the PUU/IPSW biofoam samples were ground into powders and then plated with gold and subjected to 10kV voltage. Prior to the test, the samples' surfaces were gold-plated in order to have conductive properties and to be detectable by the SEM detector Phenom ProX secondary electron detector (SED).

Fourier transform infrared spectroscopy

The PUU/IPSW biofoam chemical structure was analyzed with FTIR spectroscopy by using KBr pellet technique with measurements at 3500-400 cm^{-1} wavenumber.

Thermogravimetric analysis

The PUU/IPSW biofoam was subjected to TGA to obtain its thermal resistance with the TGA DSC 200 of Seiko SSC 5200H at a temperature of 25-600 (°C) with a heating rate of 10°C/minute.

Impedance tube testing

The PUU/IPSW biofoam sound-proofing ability was measured with an acoustic test that followed the ASTM E-1050 standard. The biofoam samples were shaped into a 28mm-diameter circle. Two microphone techniques and automated frequency analysis systems were used to quantify the effect of normal sound absorption coefficient and precise normal acoustic impedance comparisons of materials, with frequencies ranging from 0 to 6400 (Hz) [10, 11,15].

Results and Discussion

Cell morphology

Two microscopes, SEM for 500x magnification (Figure 2) and Microscope Camera for 10x magnification (Figure 3), were used to examine the biofoam pore morphology. Three samples, namely BP0, BP5, and BP1.5 were observed on SEM as representative treatments. The results show that majority of the pores formed were macropores since the size was found to be more than 50µm. Three types of biofoam morphology were then determined: 1) open-celled, meaning that the biofoam pores were found to have interconnecting holes between each other; 2) closed-celled, meaning that the biofoam pores were found to not have interconnecting holes between each other; and 3) intermediate-celled, meaning that the biofoam pores were found in a combination of the two. BP0 was found to be closed-celled, with circular to oval shape when it expanded. BP5 was found to be

intermediate-celled with oval shape [3]. Other microstructures were observed in PU layers. BP1.5 had closed-celled microstructure with polygonal shape. It had another microstructure, namely interconnecting hole. According the SEM images, filler addition influenced the biofoam morphology. It was observed that the filler could make a closed-celled sample to be an open-celled one, since it filled the biofoam matrices. Meanwhile, the effect of filler addition to MDI ratio enhancement was found to be not significant. The SEM image results were smooth, demonstrating MAH's ability to act as a coupling agent. The smoothest the sample captured by SEM causes the role of MAH which can relate the filler and the biofoam matrices. Therefore, the surface of samples seemed smooth.

The structure of the cavities and pores created during the polymerization process and the cell size were determined by the gelling and blowing reactions. If the cavity pressure is greater than the wall strength, biofoam with an open-celled structure may be created. At low channel flow rates, the cavity wall thickness retains hardness. However, if the hardening process is completed before the open pore formation, some open pores can form. Closed cells will remain if the cavity wall hardens completely before fracturing [2, 16, 17]. With the addition of filler, the pore distribution continued to reduce in size (Figure 3). It was identified that sample BP0 had the highest pore distribution with pore size in the range of 250-300 µm, while Samples BP1, BP3, BP4, BP5, and BP1.5 had pore sizes in the range of 100-150 µm. Meanwhile, Sample BP2 had pore distribution with pore size in the range of 150-200 µm. The factor which caused different sizes of pore distribution might occur when the minimum biofoam synthesis period and stirring velocity were not fulfilled. It was suggested that foaming under this kind of condition impacted the cell sizes of Sample BP2. This demonstrated that the presence of filler had a direct impact on the morphological properties and distribution. The biofoam mechanical and thermal efficiency depended on these factors [8].

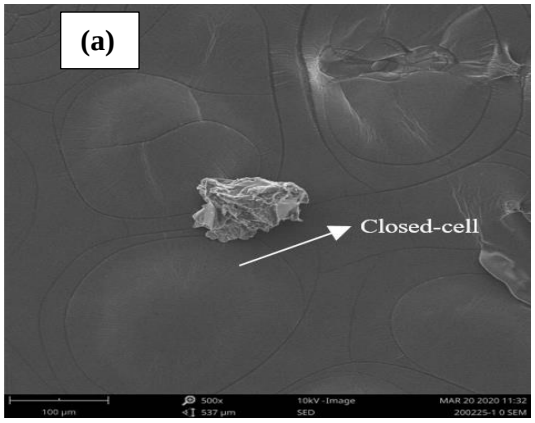

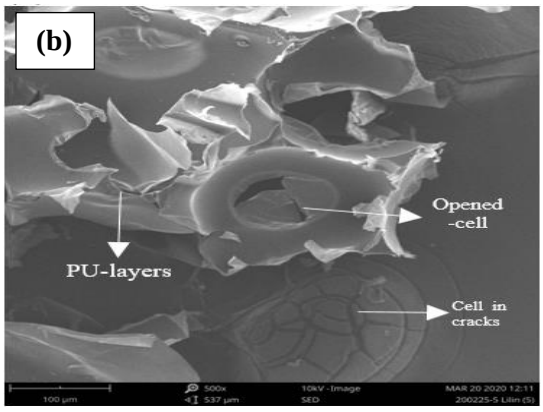

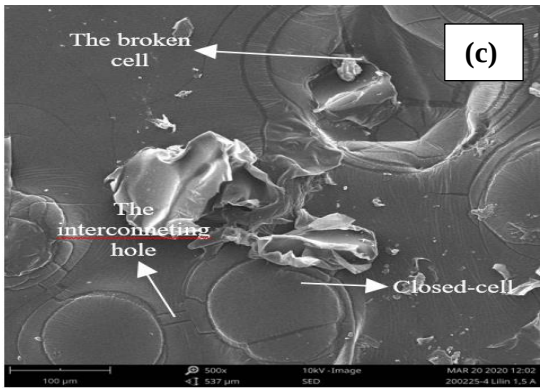

Figure 2. SEM images from the PUU/IPSW biofoam samples of (a) BP0, (b) BP5, and (c) BP1.5.

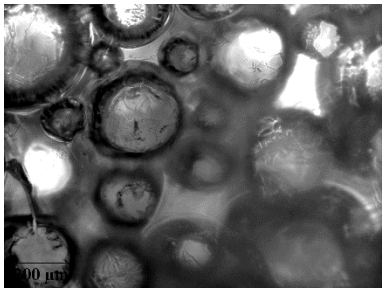

(BP0)

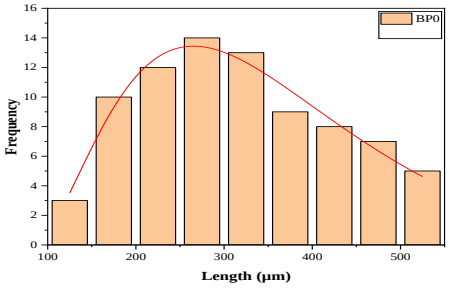

(BP0)

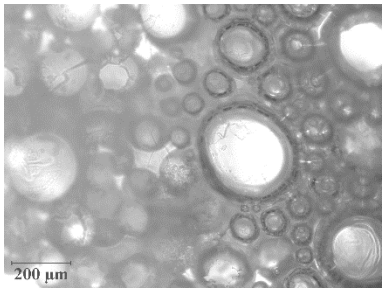

(BP1)

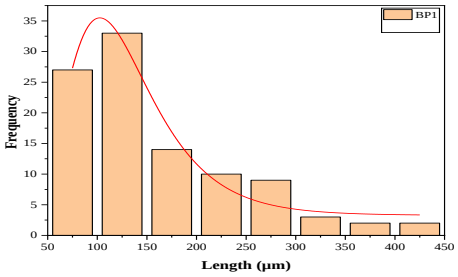

(BP1)

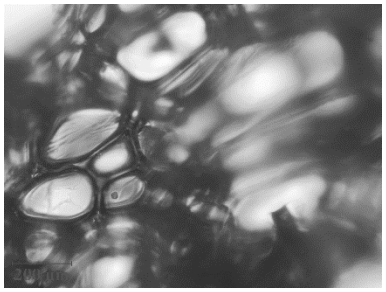

(BP2)

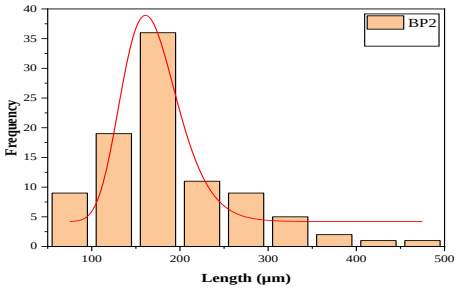

(BP2)

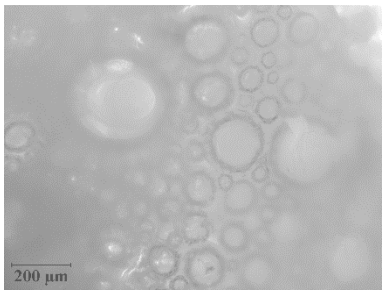

(BP3)

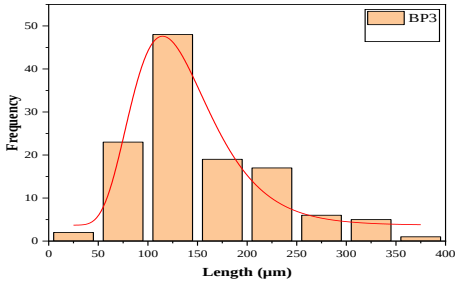

(BP3)

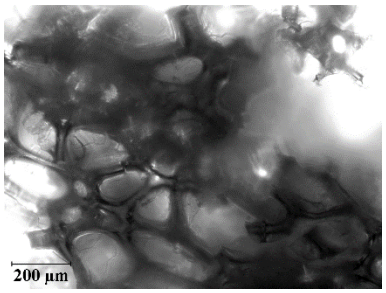

(BP4)

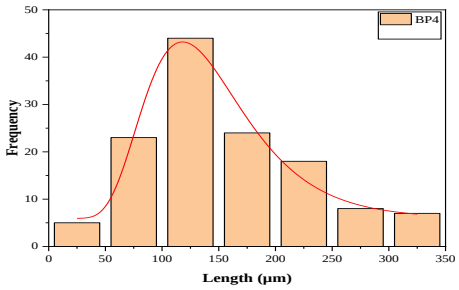

(BP4)

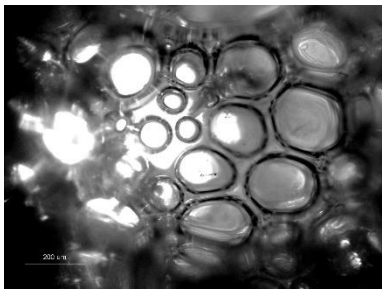

(BP5)

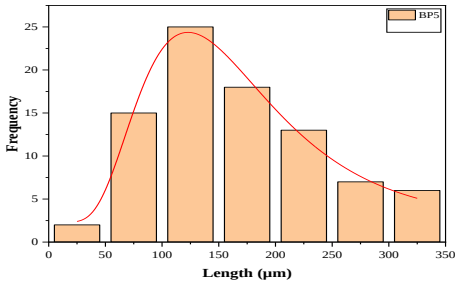

(BP5)

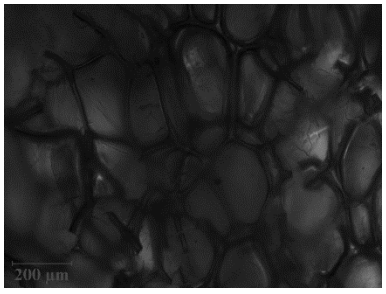

(BP1.5)

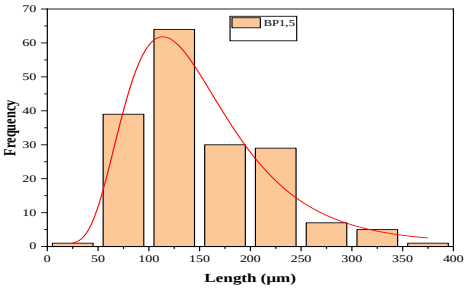

(BP1.5)

Figure 3. The PUU/IPSW biofoam microscope camera profile and pore distribution curves

Chemical structure

Urethane and urea are two forms of carbonyl groups formed by hydrogen bonds [18]. The PUU biofoam is derived from polyol and diisocyanate raw materials. Samples of MDI, PEG, BP0, and BP5 were observed to understand the PUU/IPSW biofoam chemical reaction. According to the absorption observed in the FTIR spectra, the -NH functional group was found in the wavenumber range of 3808-3308 cm^{-1} with broad intensity. This covered Samples BP0 (3516 cm^{-1}) and BP5 (3527 cm^{-1}). Samples BP0 (3382 cm^{-1}), MDI (3384 cm^{-1}) and BP5 (3382 cm^{-1}) belonged to -OH functional group found in the wavenumber range 3422-3314 cm^{-1}. The absorption peak of the PUU biofoam formed shifted to a lower wavenumber, suggesting a looser bond [13, 19]. Methylene functional group was detected at the absorption peak wavenumbers of 2972 cm^{-1} and 2971 cm^{-1} which was the -CH asymmetric stretching vibration of CH_3 [9, 19].

The absence of an isocyanate functional group absorption band at wavenumbers 2270-2250 cm^{-1} suggested that the isocyanate reacted properly with polyol (Figure 4). The first explanation is that due to the steric disturbance molecule, the -OH functional group interacted with the -NCO group. Another explanation is that the –NCO functional group interacted with the –OH group in the air, which was caused by humidity [6, 20]. The characteristics of amide III and C = O (-RNHCOO- / urethane linkage) functional groups in the absorption bands of 1230 cm^{-1} and 1077 cm^{-1} suggested that the PUU biofoam was successfully formed and chemically bonded [6, 19, 21]. In addition, another absorption peak was detected, namely the aromatic group C-C/C = C stretching modes in the wavenumber range 1600-1607 cm^{-1} [22]. The properties of EDA as a chain extender contributed to the PUU biofoam's hard segment character, which can be detected when the biofoam is heated or cooled. When PUU biofoam is heated to a specific temperature, it has a peak intensity –H bonded urethane C = O groups while urea groups decrease. This also applies if it is cooled to a temperature of 120-30 (°C) so that the peak intensity of -H bonded urethane C=O groups increases while the peak intensity of free urethane C=O decreases [18]. More information is presented inTable 2.

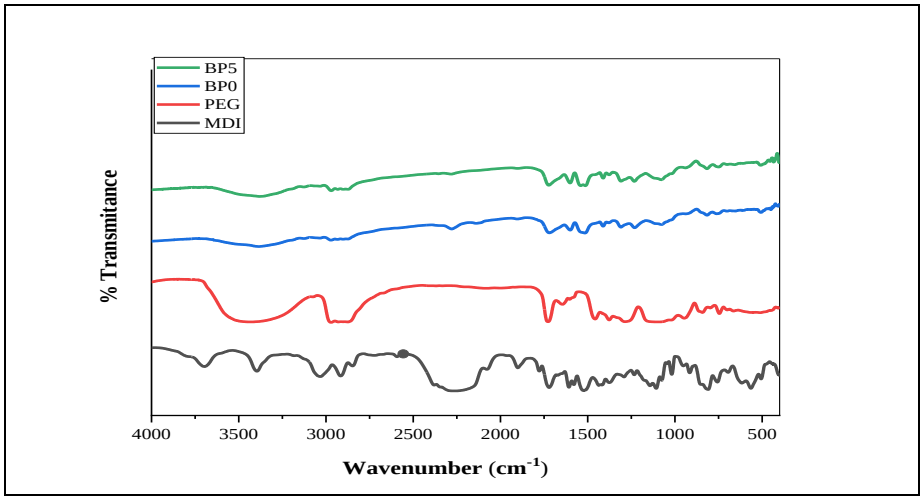

Figure 4. FTIR spectra of BP0, PEG, and MDI

Table 2. Peaks of FTIR spectra of BP0, PEG, and MDI

Wavenumber (cm^{-1})				Wavenumber Range (cm^{-1})	Functional Groups
MDI	**PEG**	**BP0**	**BP5**		
-		3516	3527	3808-3308	The stretching vibration of -NH
3384	-	3382	3382	3422-3314	-OH stretching modes from hydroxy groups
-	2972	2972	2971	3000-2970	-CH asymmetric stretching vibration CH_3 (methylene groups)
2257	-	-	-	2270-2250	-NCO- (isocyanate asymmetric stretching)
1720	-	1719	1724	1724-1705	Disorder H-bonded (C=O)OC in urethane
-	1644	1638	1635	1648-1627	Order H-bonded urea C=O
1607	1602	1600	1600	1615-1580	Aromatic C-C/C=C Stretching Modes
1233	-	1230	1230	1257-1222	υC-N+ δN-H (Amide III)
1075	-	1077	1075	1083-1070	H-Bonded (C=O)OC in urethane

TGA analysis

Thermogravimetric Analysis (TGA) is used to calculate the effect of filler addition (industrial plywood sawdust waste) and the ratio of MDI to its thermal performance, while DTG is a derivative of its mass loss. Samples BP0, BP5, and BP1.5 were observed because they were representatives to the treatment. Figure 5 and Table 3 show the results of the TG and DTG tests. Temperature characteristics were divided into T_{Onset} and T_{max}. T_{Onset} was the degradation of temperature when the mass loss was 5%, while T_{max} was the maximum degradation temperature of all samples [6]. All samples had T_{max} which was divided into three stages. Before the samples were degraded at the T_{Onset} temperature in the initial stage, there was a small degradation below 100ºC which was the degradation of moisture, solvent light organic molecules, and impurities from the biofoam [23]. The T_{Onsets} of the three samples were all above 120 ºC, with BP1.5 having the highest value of 130 ºC. The first and second stages of degradation occurred at temperatures of 190-209 (ºC) and 294-295 (ºC) respectively, and involved the decomposition of polymer urethane bonds [7, 13, 21]. The last degradation that occurred was the soft segment decomposition of the MDI biofoam at a temperature above 500ºC. This stage involved combustion and aromatic oxidation [7, 24], as well as the degradation of lignin (industrial plywood sawdust) and other molecules that were difficult to separate from the previous stage [21, 25]. Furthermore, the DTG curve (Figure 5) shows that the greatest mass loss occurred at 294 ºC which was the hard segment decomposition stage while the temperature above 525 ºC was the soft segment decomposition stage.

Figures 5(a)-(c) show the TGA results. It was found that BP0, or the biofoam without the addition of waste or MDI ratio, had better thermal resistance. This is because its thermal degradation profile showed that mass loss generally occurred at higher temperature compared to BP1 and BP1.5 (Figure 5 (a)). When biofoam filler was added, it is suggested that two things might have occurred: 1) the organic filler might contain a small amount of water residue as a result of the formation of urea bonds which increases the activation energy for thermal degradation [8], or 2) the addition of filler improved strength by giving the part a hard segment character, which increased thermal resistance [23]. Based on the results found, it should be the result that led to the second reason but this research showed that BP0 had highest thermal conductivity. It means that the filler-free biofoam had good thermal resistance. Another factor that caused a decrease in thermal performance was the uneven distribution of the filler in the polymer matrix which affected density. Besides, the TGA results were also influenced by pore

morphology. The modified biofoam's high pores and open cavities hastened the degradation process, thus reducing the thermal efficiency of the substance being analyzed [8].

DSC analysis was used to measure the change in mass of the heat-treated samples. TGA cannot normally detect physical changes in polymer structures such as glass transition, crystallization, or melting, but these can be determined through DSC [23]. The DSC analysis (Figure 5) reveals that none of the biofoam samples had endothermic melting peaks. This could be caused by a physical changeover of the polymer, or the density from melting at a fast cooling rate to a glassy amorphous state or impure samples. Samples B5 and BP1.5 had a single exothermic peak at 522 °C and 538 °C respectively, while Sample BP0 had two exothermic peaks at 539 °C and 551 °C.

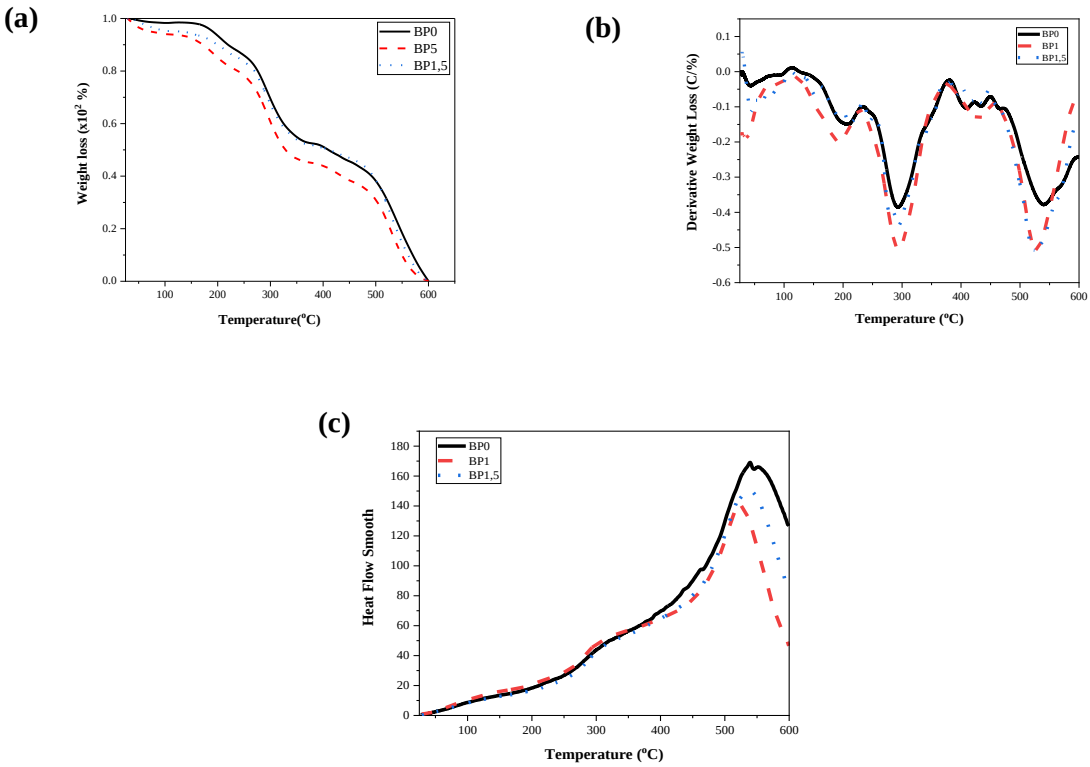

Figure 5. TGA (a), DTGA (b), and DSC (c) of the PUU/IPSW biofoam

Table 3. The sections of thermal degradation on the PUU/IPSW biofoam

Sample Codes	T_{onset} (°C)	(Stages) T_{max} (°C)			Residual Mass 600 °C (%)
		I	II	III	
BP0	126	206	294	539	37.29
BP5	130	190	295	528	23.00
BP1.5	130	209	294	527	33.48

Sound absorption coefficient

The sound absorption coefficient (α) for all samples is shown in Figure 6. The three samples (BP0, BP4, and BP1.5) were measured in the wavenumber range of 0-6400 (Hz) with two microphone impedance tubes and with similar sample thickness of 1.5 cm. Sample BP4 was selected as the representative to the treatment for 1:1 ratio, and the addition of IPSW with highest SAC compared to the other samples. The detailed information regarding SAC for all samples can be found in previous publication [12]. The results showed that BP4 had the highest sound absorption, with a value of 0.69 at 3864 Hz, followed by BP0 with a value of 0.65 at 4552 Hz, and BP1.5 with a value 0.45 at 4760 Hz. All samples showed the best acoustic performance at high frequencies above 3800 Hz. Based on these results, it was found that BP4 had the best acoustic performance, showing that that of BP0 and BP1.5 was not optimal. The addition of filler to the synthesis of polyurethane foam can enhance sound absorption [10, 11]. But this did not apply to the PUU/IPSW biofoam sample with IPSW of above 4% [12] and did not enhance MDI ratio. Several other factors influenced the biofoam sample ability to absorb sound which are explained in the following.

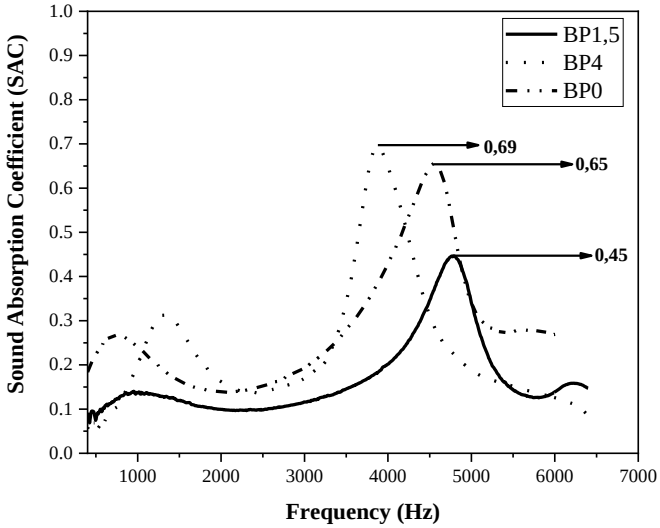

Figure 6. The PUU/IPSW biofoam sound absorption coefficient

Effect of texture, pore morphology, and density

Sound-absorbing foam will have a high SAC value if it has the following material characteristics [20, 25, 26]:

1. Flexible foam texture
2. Open-celled microstructure
3. Small-sized pores in large numbers
4. Higher density (not measured in this research)

The synthesized PUU/IPSW biofoam had the characteristics of semirigid texture, intermediate microstructure, smaller pore size, and higher SAC value than the control biofoam. This can be caused by other influencing factors such as the characteristics of the pores. Even if the size is small and numerous, it may not meet aspects such as structure and pore characteristics of sound-absorbing materials, including those mentioned below [17].

1. The material contains several pores and holes, all of which are small and uniform in size
2. The pores and holes must be connected.
3. The pores and holes inside the material must connect with the outer surface.

Effect of filler addition

The biofoam filler used, called IPSW, was measured by 30 mesh size. The filler had an impact on pore size in such a way that biofoam with added filler had smaller pores than those without filler addition. The smaller pore size was closely related to improved sound absorption mechanism. It is suggested that smaller pores allowed sound waves to dissipate sound energy and dampened it as they move through the sound-absorbing material. Therefore, smaller pores in large numbers allowed more sound wave to collide with the cell wall, lengthening the reflection & bending portion and causing more energy to be absorbed, resulting in higher SAC [10, 15, 20, 27]. The smaller pore size in the synthesized biofoam is shown in Figure 3. The existence of other factors that predominantly affect sound absorption such as the unfulfilled criteria for pores as sound absorbers had resulted in the reduced acoustic performance of the PUU/IPSW biofoam. However, if adjusted and designed with a better formula, the PUU/IPSW biofoam had a great potential as a noise-absorbing material with wide range frequency.

Effect of MDI ratio enhancement

Isocyanate (MDI) is composed of hard segment. Enhancing the MDI ratio can reduce SAC, as shown in Sample BP1.5. Biofoam with added MDI ratio had leaning rigid texture. The texture rigidity was caused by the closed-celled microstructure. Another factor which could make the biofoam texture rigid was chain extender [19, 20].

Conclusion

The PUU/IPSW biofoam was successfully synthesized after its functional groups (–NH, -OH, -CH, -CO and C-C) were identified in the FTIR spectra. Addition of filler and increase in MDI affect pore morphology, thermal resistance, and acoustic performance. Samples BP0 and BP1.5 of the synthesized biofoam had close-celled microstructure morphological type while Sample BP5 had intermediate-celled type. All samples had thermal resistance above 120 ^{o}C. Sample BP4 had the highest SAC with the value of 0.69. The acoustic output was poor, resulting in lower-frequency SAC when tested. However, if adjusted and designed with a better formula, PUU/IPSW biofoam can absorb sound at wide-range frequency. Lastly, filler addition could enhance the biofoam property performance. Therefore, IPSW is promotable as an organic filler for renewable material.

Acknowledgement

The authors thank Rosid Eka Mustofa for assisting with the OriginLab analysis, Iklima Maharani for directing the sample preparation stages, Safira C for laboratory access to the Microscope Camera tool, and all SEM, TGA, FTIR, and Acoustic laboratory test equipment operators who tested all samples in this research.

References

1. Aditya, V. T., Masykuri, M. and Setyono, P. (2019). Analysis of noise in the green open space Putri Kaca Mayang, Pekanbaru City. *AIP Conference Proceedings: International Conference on Biology and Applied Science (ICOBAS)*, 2019.040020.
2. Cao, L., Fu, Q., Si, Y., Ding, B. and Yu, J. (2018). Porous material for sound absorption. *Composites Communications*, 10(2018): 25-35.
3. Rojo-Gomez, R., Alameda, L., Rodriguez, A., Calderon, V. and Guiterrez-Gonzalez, S. (2019). Characterization of polyuretane foam waste for reuse in eco-efficient building materials. *Polymers*, 11: 359.
4. Gama, N.V., Ferreira, A. and Timmons, A. B. (2018). Polyurethane foams: Past, present and future. *Materials*, 11(10) : 1-35.
5. Akindoyo, J. O., Beg, M. D. H., Ghazali, S., Islam, M. R., Jeyaratman, N. and Yufaraj, A. R. (2016). Polyurethane types, synthesis and applications- a review. *Royal Society of Chemistry*, 6(1) : 114453-114482.
6. Alis, A., Majid, R. A., and Mohammad, Z. (2019). Morphologies and thermal properties of palm-oil based rigid polyurethane/halloysite nanocomposite foam. *Chemical Engineering Transactions*, 72(2019): 415-420.

7. Bundjali, B., Masykuri, M., Hartanti, F. W. and Arcana, I. M. (2018). Poly (urethane-urea) synthesized from 9-ethoxy-1, 10-octadecanediol obtained by modification of palm oil oleic acid. *Journal of Mathematics and Fundamental Sciences*, 50(1): 13-27.
8. Czlonka, S., Strakowska, A., Strzelec, K., Kairyte, A., and Kremensas, A. (2020). Bio-based polyurethane composite foams improved mechanical, termal, and antibacterial properties. *Materials*, 13(1):1-20.
9. Chen, X., Xi, X., Pizzi, A., Fredon, E., Zhou, X., Li, J., Gerardin, C. and Du, G. (2020). Preparation and characterization of condensed tannin non-isocynate polyurethane (NIPU) rigid foams by ambient temperature blowing. *Polymers*, 12(4):1-20.
10. Azahari, M. S. M., Rus, A. Z. M., Kormin, S. and Zaliran, M. T. (2017). Acoustic properties of polymer foam composites blended with different percentage loadings of natural fiber. *IOP Conferences Series: Materials Science and Engineering*, 244(2017):1-6.
11. Azahari, M. S. M., Rus, A. Z. M., Kormin, S. and Zaliran, M. T. (2018). An acoustic study of *Shorea leprosula* wood fiber filled polyurethane composite foam. *Malaysian Journal of Analytical Science*, 22(6): 1031-1039.
12. Nofitasari, H., Masykuri, M. and Ramelan, A. H. (2020). Reducing room noise using polyurethane-urea biofoam/industrial plywood sawdust waste (PUU/IPSW). *AIP Conferences Proceedings: International Conference on Science and Applied Science*, 2296(2020): 020061-020066.
13. Czlonka, S., Strakowska, A., Strzelec, K., Kairyte, A., and Vaitkus, S. (2019). Composites of rigid polyurethane foams and silica powder filler enhanced with ionic liquid. *Polymer Testing*, 75(2019) : 12-25.
14. Mustafov, S. D., Sen, F. and Seydibeyoglu, M. O. (2020). Preparation and characterization of diatomite and hidroxyapatite reinforced porous polyurethane foam biocomposites. *Scientific Reports*, 1(2020): 1-9.
15. Rus, A. Z. M. and Shafizah, S. (2015). Acoustic behavior of polymer foam composite of *Shorea leprosula* after UV-irradiation exposure *International Journal Mechanical Aerospace, Industry Mechatronics*, 9(2015) :188-192.
16. Sung, G., Kim, S. K., Kim, J. W. and Kim, J. H. (2016). Effect of isocyanate molecular structures in fabricating flexible polyurethane foams on sound absorption behavior, *Polymer Test*, 53(2016): 156-164.
17. Zhao, C., Wang, P., Wang, L. and Liu, D. (2014). Reducing railway noise with porous sound-absorbing concrete slabs. *Advance Material Science Engineering*, 2014: 1-11.
18. Kayalvizhi, M., Vakees, E., Suresh, J. and Arun, A. (2019). Poly(urethane-urea) based on functionalized polystyrene with HMDI: Synthesis and characterization. *Arabian Journal of Chemistry*, 12(8) : 2484-2491.
19. Jiang, L., Ren, Z., Zhao, W., Liu, W., Liu, H. and Zhu, C. (2018). Synthesis and structure/properties characterizations of four polyurethane model hard segments. *The Royal Society Open Science*, 5(7): 1-11.
20. Tiuc, A. E., Vasile, O., Usca, A-D., Gabor, T. and Vermesan, H. (2014). The analysis of factors that influnce the sound absorption coefficient in porous materials. *Romanian Journal of Acoustics and Vibration*, 11 (2):105-108.
21. Zhao, X., Qi, Y., Li, K. and Zhang, Z. (2019). Hydrogen bonds and FTIR peaks of polyether polyurethane-urea. *Key Engineering Materials*, 815(2019):151-156.
22. Bayu, A., Nandiyanto, D., Oktiani, R. dan Ragadhita, R. (2019). How to read and interpret FTIR spectroscope of organic material. *Indonesian Journal of Science and Technology*, 4(1): 97-118.
23. Ng, H. M., Omar, F. S., Saidi, N. M. and Kasi, R. (2018). *Encyclopedia of Polymers Science and Technology*. Jhon Waley Sons Inc, New York: pp. 1-29.

24. Kripluks, M., Cabulis, U., Ivdre, A., Kuranska, M., Zileniewska, M. and Auguscik, M. (2016). Mechanical and thermal properties of high-density rigid polyurethane foams from renewable resources. *Journal Renewable Material*, 4(1): 86-100.
25. Huang, X.Y., Hoop, C. F., Peng, X. P., Xie, J. L., Qi, J. Q., Jiang, Y. Z., Xiao, H. and Nie, S. X. (2018). Thermal stability analysis of polyurethane foams made from microwave liquefaction bio-polyols with and without solid residue. *BioResources*, 13(2): 3346-3361.
26. Amares, S., Sujatmika, E., Hong, T. W., Durairaj, R. and Hamid, H. S. H. B. (2017). A review: characteristic of noise absorption material. *IOP Conferences Series: Journal of Physics: Conferences Series*, 908(2017): 012005.
27. Hassan, N. N. M. and Rus, A. Z. M. (2016). Influences of thickness and fabric for sound absorption of biopolymer composite. *Applied Mechanics and Materials*, 393(1): 102-107.